Acoustics 2021
Wollongong, Australia
MAKING WAVES

Application of Wall-Modelled LES to the Prediction of Turbulent Flow Noise

Graeme Lane (1, 2), William Sidebottom (2, 3) and Paul Croaker (2)

(1) Mechanical and Automotive Engineering, RMIT University, Melbourne, Victoria, Australia
(2) Maritime Division, Defence Science and Technology Group, Fishermans Bend, Victoria, Australia
(3) University of New South Wales, Sydney, NSW, Australia

ABSTRACT

Large eddy simulation (LES) has the potential to be a high-fidelity approach for predicting broadband noise from turbulent boundary layer flow, with the predicted surface pressure fluctuations providing an input to acoustics analogies. However, the practical application of conventional wall-resolved LES is limited by high computational cost. Therefore, wall-modelled LES (WMLES) has been investigated as a means to reduce this cost. Simulations were carried out using OpenFOAM, with channel flow as a test case. Predictions from both wall-resolved and wall-modelled approaches were compared against data from direct numerical simulation (DNS). The accuracy of WMLES was found to be comparable to that of wall-resolved LES over most of the channel, while incurring less than a tenth of the cost. However, near-wall accuracy of the boundary layer statistics from WMLES was reduced, resulting in a reduction in accuracy for the estimated wall pressure fluctuations. As an alternative approach, a semi-analytical method has been tested, which does not rely on the pressure fluctuations. Instead, a model derived from a Fourier transform solution of the pressure Poisson equation was implemented, with the boundary layer parameters supplied by LES. The accuracy of the resulting spectra for each LES method is discussed.

1 INTRODUCTION

Prediction of noise from turbulent flow is of interest in a wide range of applications. Examples include the noise generated by wind turbines, propellers, fans, aircraft wings, and the flow around marine vehicles. One approach to quantifying such noise emissions is the two-stage combination of large eddy simulation (LES), to predict the near-field fluid flow, in combination with an acoustics analogy (such as the Ffowcs Williams and Hawkings (FWH) model) to predict the far-field sound levels. LES explicitly resolves the larger, energetic eddy structures in a turbulent flow, and its output includes predictions of pressure fluctuations that can be used as a basis for acoustics predictions. However, adoption of this approach as an everyday engineering design tool is severely compromised by the very high computational cost of conventional LES. As a result, there is interest in modified LES methods which can reduce this cost. One such approach is wall-modelled LES (WMLES). In the present study, the suitability of WMLES as a basis for acoustics predictions has been assessed.

Various studies have been reported in the literature demonstrating the application of LES to acoustics predictions. For example, Wolf and Lele (2012) applied LES to predict the flow around a NACA0012 aerofoil. The FWH analogy was then used to predict the far-field sound spectrum based on integration of the dipole sources over the surfaces of the aerofoil. Winkler et al. (2020) simulated the flow around a NACA 6512-63 airfoil, and predicted the acoustic far-field based on either the FWH or Amiet analogies. In these studies, however, the computational cost is very high, since conventional, wall-resolved LES (WRLES) was employed. The difficulty arises because with wall-bounded turbulent flow, turbulence structures diminish in size as a wall is approached, but they must still be resolved by a mesh. This leads to requirements for a highly-refined mesh near the wall. Also, the small cell size near walls reduces the allowable time step of the transient simulation. As the Reynolds number of a flow configuration increases, the ratio of largest to smallest eddy sizes increases, and the number of cells required for LES grows rapidly, at approximately $\mathrm{Re}^{1.85}$ (Choi & Moin, 2012). As a result, conventional LES is not affordable for full-scale applications, where Reynolds numbers are high.

WMLES can provide a more affordable alternative to WRLES. In the wall-modelled approach, no attempt is made to resolve the small eddies near the wall, thus avoiding the need for near-wall mesh refinement. Instead, only the eddies in the outer 90% or so of the boundary layer thickness are resolved, while the effects of the missing “inner” layer are accounted for through a mathematical model which imposes the correct wall shear stress in the absence of near-wall eddies. Through reduction in the overall mesh size and the resulting increase in the allowable time step, this approach can lead to cost savings of orders of magnitude.

The WMLES approach has also been used in a number of studies, to predict wall pressure spectra and related far-field noise. For example, Park and Moin (2016) applied a WMLES method using the CharLES code to simulate turbulent channel flow, and obtained good predictions of the power spectral density (PSD) of the wall-pressure fluctuations. George and Lele (2016) used the Vida code to simulate flow around a NACA0012 aerofoil, and obtained good predictions for wall pressure spectra and far-field sound pressure level. Mehrabadi et al. (2019) also applied WMLES to study flow over a NACA0012 airfoil. They obtained good predictions of the far-field sound pressure level using Amiet's model. Pérez Arroyo et al. (2019) applied WMLES using the TurboAVBP code to simulate a turbofan. Predictions of far-field using the FWH analogy were higher than experimental measurements, while better agreement was obtained using Goldstein's analogy for noise in a duct. Boukharfane et al.(2020) applied the CharLES code to simulations of a controlled-diffusion aerofoil, and showed that predictions of wall pressure spectra agreed well with experimental measurements. They also applied WRLES to the same configuration, and found that wall-modelling reduced the computational cost by a factor of about 50.

This paper reports on a study also using the WMLES approach, with the aim of making acoustic-related predictions. Simulations have been carried out using the free, open-source OpenFOAM software. Although WMLES methods have previously been reported in the literature, as mentioned above, it has been found that the appropriate settings for WMLES may in some respects be code-dependent. As published studies have been based on other software, it was found necessary to make a further assessment of the optimal settings based on the use of OpenFOAM. The investigation was based on simulations of turbulent channel flow. Although being a relatively simple and idealised flow configuration, this configuration provides a means for more rapid assessment of modelling methods, compared to simulating an aerofoil, for example. With channel flow, there is no far-field to simulate, leading to smaller meshes, and analysis is simplified due to homogeneous flow statistics in wall-parallel directions. For comparison, wall-resolved LES of the channel flow has also been carried out, allowing an assessment of relative accuracy and corresponding computational costs. Accuracy of the simulation methods has been assessed by reference to direct numerical simulation (DNS) data for this configuration according to Lee and Moser (2015).

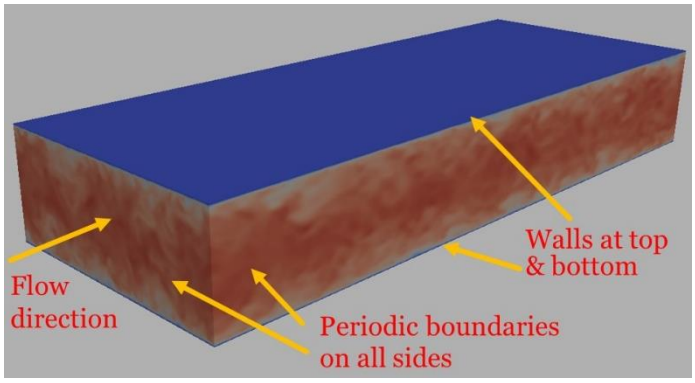

Figure 1 Schematic of channel flow setup, with contours of instantaneous velocity magnitude plotted on boundaries for WMLES case.

The simulation results presented in this paper show that the wall-modelled method can achieve a similar level of accuracy compared to wall-resolved LES in many respects, at a fraction of the computational cost. However, it was also found that predictions from WMLES for fluctuating pressure at the walls were less satisfactory. As an alternative approach for acoustics predictions, a semi-analytical model for predicting wall pressure spectra has been investigated. This approach is based on obtaining a solution to the Poisson equation which relates pressure fluctuations in a turbulent boundary layer to the velocity field. A recent treatment by Grasso et al. (2019) has been considered here. The model makes use of several parameters from the LES solution which can be more reliably calculated than the pressure fluctuations. Resulting spectra from WRLES and WMLES have been compared against DNS data.

2 SIMULATION METHOD

Simulations of turbulent channel flow were carried out using OpenFOAM (version 5.*x*) to solve the spatially-filtered, unsteady Navier-Stokes equations. The fluid was assumed to be incompressible and isothermal. Figure 1 shows the general scheme for setup of the simulations. The overall extent of the computational domain was 12.8δ x 2δ x 4.8δ in the streamwise, wall-normal and spanwise directions respectively (where δ is the channel half-height, which was set equal to 1 m). Periodic boundaries were applied in the streamwise and spanwise directions, while a zero-slip condition was assumed for the upper and lower walls. Flow in the streamwise direction was achieved by imposing a body force to maintain a uniform streamwise pressure gradient. The source term automatically adjusts at each time step to maintain a specified bulk velocity, which was set to 0.28 m/s. The kinematic viscosity was assumed to be 1.4×10^{-5} m^2/s, and the density was 1 kg/m^3, giving a bulk Reynolds number of 2×10^5. The friction velocity-based Reynolds number was Re_τ =1000, corresponding to a friction velocity of 0.014 m/s.

LES was carried out using both wall-resolved and wall-modelled approaches. Some of the settings were the same for both methods, including the use of a 2nd-order backward differencing scheme for time stepping, and a maximum Courant number of about 0.4. The WALE model (Nicoud & Ducros, 1999) was applied as the subgrid-scale viscosity model. Simulations were run for at least 3 flow-past times to eliminate the influence of initial conditions, before restarting statistics. For WMLES, steady-state statistics were collected for at least 10 flow-past times. For WRLES, about 5 flow-past times were used for calculating statistics, due to higher computational expense.

2.1 Method for wall-resolved simulations

A mesh with hexahedral cells was constructed following the specification given by Komen et al. (2017) for their "30-Grid". This mesh arrangement was chosen as good levels of accuracy were obtained in the study of Komen et al. (2017), who also used OpenFOAM to simulate channel flow. The mesh is specified in "inner" units, and features near-wall refinement to resolve the small eddies in the inner layer. The cells closest to the wall have a non-dimensional height $y^+ = y\,u_\tau/\nu = 0.5$, where y is the wall-normal distance, u_τ is the friction velocity, and ν is the kinematic viscosity. Wall-normal spacing increases from the first cell with a geometric ratio of about 1.07, until the spacing reaches $\Delta y = 0.02\delta$, after which it is uniform. The total number of cells used for the WRLES analyses was 33 million. For further details about the mesh, see Table 1. For WRLES, central differencing was used as the numerical scheme for the convection term in the Navier Stokes equations.

2.2 Method for wall-modelled simulations

With WMLES, no attempt is made to resolve turbulence structures in the inner part of a boundary layer, and so the mesh can have uniform spacings in the wall-normal direction. Following the recommendations of Rezaeiravesh et al. (2019), an isotropic mesh was generated, with 28 cells over a distance equal to one boundary layer thickness (or half of the channel height) in each coordinate direction. With this approach 2.6 million cells were used for the WMLES analyses. Also, because small near-wall cells are avoided, a larger time step could be used.

Because turbulent eddies in the "inner" layer are not resolved, the wall friction will be inaccurate, unless corrective action is taken. The issue is addressed by providing a wall-stress model. In the current approach, it is assumed that the mean velocity profile normal to the wall can be described by an algebraic equation, or "Law of the Wall". The streamwise velocity was assumed to conform to Spalding's equation (Spalding, 1961), and so, by sampling the velocity field near the wall, the local mean wall shear stress can be inferred. This shear stress is then enforced as a boundary condition, by setting a turbulent viscosity at the wall. Following the recommendation of Larsson et al. (2016), velocities were sampled away from walls, in order to avoid the errors typically inherent in velocity values closest to the surfaces. In the present work, velocity was sampled at the fourth cell from each surface.

Simulation results using WMLES have been found to be very sensitive to the numerical schemes, especially the scheme applied for the convection term in the Navier Stokes equations. Rezaeiravesh et al. (2019) have suggested that a moderately dissipative scheme is better compared to central differencing, which is conventionally applied in WRLES. Further investigations were carried out during the present study to test alternative differencing schemes. It was confirmed that for the 'bulk' of the channel away from the wall, the LUST (Linear Upwind Stabilised Transport) scheme produced more accurate results than central differencing. However, close to the walls, central differencing was more accurate. This led to the development of a "hybrid" differencing scheme, where central differencing is used close to the walls, while LUST is selected for the interior flow. The schemes are blended linearly across five cells in the wall-normal direction.

2.3 Semi-analytical approach for wall pressure spectra

As described in Section 3, the wall-modelled approach reduced the accuracy of near-wall pressure fluctuations. Therefore, with the aim of obtaining improved predictions of wall pressure spectra, an alternative semi-analytical approach was investigated. The approach is based on a solution to the Poisson equation relating fluctuating pressure to the velocity field, as derived by Grasso et al. (2019) for a turbulent boundary layer. Power spectral density (PSD) of wall pressure fluctuations was evaluated from the resulting mathematical model with the input of turbulence statistics through the boundary layer extracted from the LES solution. It is important to note that the LES pressure data is not required for the mathematical model of Grasso et al. (2019).

The Poisson equation is derived by taking the divergence of the momentum conservation equation for an incompressible fluid, introducing Reynolds decomposition into mean and fluctuating quantities, then subtracting the time-averaged equation. This leads to an equation of the form:

$$\frac{1}{\rho}\Delta p = -2\frac{\partial u_j}{\partial x_i}\frac{\partial U_i}{\partial x_j} - \frac{\delta^2}{\partial x_i \partial x_j}\left(u_i u_j - \overline{u_i u_j}\right) \tag{1}$$

where ρ is the fluid density, p is pressure, and in the i^{th} coordinate direction, u_i is the fluctuating velocity, U_i is the mean velocity and x_i is the position vector. The righthand side contains two terms, where the first is usually referred to as the mean shear-turbulence interaction (or "fast") term, while the second describes the interaction between fluctuating velocity components only and is referred to as the turbulence-turbulence (or "slow") term. Grasso et al. (2019) took the Fourier transformation of equation (1) to obtain a modified Helmholtz equation, which was then solved in the wavenumber domain using a Green's function approach. For a complete derivation, see Grasso et al. (2019).

To evaluate the wall-pressure PSD with this model, several parameters describing the boundary layer characteristics are required as input. These include wall-normal profiles for mean velocity, gradient of mean velocity, and r.m.s. wall-normal velocity fluctuation. These quantities are readily obtained from LES and are generally quite accurate, as will be seen in the proceeding section. However, there is one remaining difficulty, which is the requirement to provide the integral length scale of turbulence, which is not a standard output of LES. A range of different methods have been suggested in the literature for estimating this length scale, but the validity of each method must be carefully considered. An additional complication is that different length scales can be calculated for different coordinate directions (Kamruzzaman, 2011). However, in the mathematical analysis of Grasso et al. (2019) it was assumed that the integral scale corresponds to an isotropic flow where there is no directional variation in turbulence statistics. Hence, in the following discussion, only the isotropic length scale has been considered.

For estimating the integral length scale in boundary layers, a reasonable starting point is the generally accepted notion (e.g. Panton & Linebarger, 1974) that, close to the wall, the integral length scale should vary approximately linearly in proportion to the distance from the wall, while in the outer part of the boundary layer, the integral length scale should be some fraction of the boundary layer thickness and approximately constant. An equation that satisfies these requirements was proposed by Michel et al. (1968):

$$\frac{\Lambda}{\delta} = \frac{\zeta}{\kappa}\tanh\frac{\xi y}{\zeta\delta} \tag{2}$$

where κ is the von Karman constant (equal to 0.41), ζ is a constant equal to 0.085, ξ is a constant equal to 0.4, and δ is the boundary layer thickness (equivalent to the channel half-height). This equation shows a linear behaviour with $\Lambda = y$, in the limit of $y \to 0$, while for $y \to \delta$, a flat "plateau" region is obtained, with a value $\Lambda \approx 0.2\delta$. However, more recent evidence from DNS (Carrara, 2016) indicates that there is no universal constant value for the plateau region. Instead, the integral scale in the outer region varies with Reynolds number, and should be estimated from the properties of the turbulent flow.

The integral length scale is also commonly calculated using an equation derived from dimensional analysis (Pope, 2000):

$$\Lambda = C\frac{k^{3/2}}{\varepsilon} \tag{3}$$

where k is the turbulent kinetic energy, $\boldsymbol{\varepsilon}$ is the specific rate of dissipation of turbulent kinetic energy, and the constant C usually has a value 0.4–0.5. This equation assumes the existence of high Reynolds number turbulence, with a large difference between the largest and smallest scales of turbulence. Such conditions only exist in the outer region of boundary layers (and even then, only for sufficiently high Reynolds number). However, there is another complication. While *k* can be estimated from LES based on the resolved Reynolds stresses, the energy dissipation, ε, is not a direct simulation output.

Due to the above difficulties, an alternative equation has been adopted in the present study for the outer region of the boundary layer, in which Λ is estimated according to (Wilcox, 1993):

$$\Lambda = \frac{1}{\kappa}\sqrt{\left|\overline{u'v'}\right| \Big/ \left|\frac{\partial U}{\partial y}\right|^2} \tag{4}$$

where $|\overline{u'v'}|$is the mean resolved Reynolds shear stress, and $\frac{\partial U}{\partial y}$ is the mean wall-normal velocity gradient. The advantage of this equation is that the required quantities are readily available from LES. However, this equation does not have the correct properties in the region close to the wall, where linear behaviour is expected. Therefore, in the final approach, equation (4) was combined with an equation for the near-wall region (y^+ <100) which has the same form as that used by Michel et al. (1968). In the present work, the constants of the Michel equation were slightly modified based on calibration using DNS data, so that $\zeta = 0.06$ and $\xi = 0.51$.

Table 1: Comparison of simulations using wall-resolved and wall-modelled approaches

	Wall-resolved LES	Wall-modelled LES
Δx/δ	0.03	0.036
Δy/δ	0.001 – 0.02	0.036
Δz/δ	0.01	0.036
Total mesh size	33 million	2.6 million
Time step (s)	0.0085	0.029
Total CPU hours	21370	1635

3 SIMULATION RESULTS

Predictions of the velocity and pressure statistics according to the wall-resolved and wall-modelled simulations are illustrated by the plots in Figure 2. Errors in the simulation results have been quantified based on a formula suggested by Rezaeiravesh et al. (2019), where the error, ϵ_∞, is defined as the maximum difference between LES and DNS values across each profile normalised by the maximum DNS value of the given parameter, g. Thus:

$$\epsilon_\infty[g] = \frac{\max|g(y) - g_{DNS}(y)|}{\max|g_{DNS}(y)|} \tag{5}$$

Figure 2(a) shows the wall-normal profile of the mean streamwise velocity. Compared to the DNS data of Lee and Moser (2015), a similar level of accuracy is obtained over most of the channel height for the two methods. For WRLES, the profile is predicted with $\epsilon_\infty = 3\%$. For WMLES, excluding the first point closest to the wall, the error is also 3%, while including the first point gives $\epsilon_\infty = 4\%$.

Figure 2(b) – 2(d) show the fluctuating velocity components in streamwise, spanwise, and wall-normal directions, For the streamwise component, the curve is predicted by WRLES with an error $\epsilon_\infty = 6\%$. Excluding the point closest to the wall, $\epsilon_\infty = 6\%$ for WMLES as well. However, including the first point from the wall, $\epsilon_\infty = 12\%$. For the spanwise component, both methods give small errors across most of the channel, except that near the wall, WRLES underpredicts the DNS curve, while WMLES overpredicts it. For WRLES, $\epsilon_\infty = 10\%$, while for WMLES $\epsilon_\infty = 12\%$ neglecting the point closes to the wall. Including this point, $\epsilon_\infty = 20\%$. For the wall-normal component of fluctuating velocity, the profile according to WRLES has an error $\epsilon_\infty = 8\%$, while for WMLES the error (including all points) is $\epsilon_\infty = 11\%$. For the Reynolds shear stress, $|\overline{u'v'}|$, shown in Figure 2(e), the error for WRLES is $\epsilon_\infty = 11\%$. WMLES gives a similar level of error across most of the profile, except for the second point from the wall, where the error is larger, so that for the overall profile $\epsilon_\infty = 28\%$.

Thus, in general, WRLES and WMLES gave a similar level of accuracy for all the statistics related to the velocity field, except that the first and second points closest to the wall introduce some additional errors for WMLES. However, it must be emphasised that the wall-modelled simulation was completed at a fraction of the cost. To achieve greater accuracy using WRLES, the computational cost was about 13 times as high (see Table 1). It should also be noted that a rather moderate Reynolds number (Re_τ = 1000) was chosen as a basis for this comparison, in order to make the WRLES computation feasible with the available computer resources. As Reynolds number increases, WRLES requires increasingly larger mesh sizes, while WMLES can keep the same mesh. As a result, the ratio of cost between WRLES and WMLES will increase rapidly for higher Reynolds numbers.

Figure 2(f) shows the predictions for r.m.s. pressure fluctuations. For y/δ > 0.15, values are fairly close to the DNS data with both methods. Excluding the points closer to the wall, $\epsilon_\infty = 8\%$ for WRLES, while for WMLES, $\epsilon_\infty = 7\%$. Closer to the wall, WRLES shows moderate underprediction, while WMLES overpredicts the DNS data. Including all points, $\epsilon_\infty = 15\%$ for WRLES, and $\epsilon_\infty = 32\%$ for WMLES. Considering only the wall-adjacent cells, the error

for WRLES reduces again, making it possible to use WRLES to give a reasonable prediction of the wall pressure spectrum. On the other hand, the maximum error in the WMLES profile occurs adjacent to the wall, and this error is also considerably larger what is seen near the wall for the mean and fluctuating velocity statistics. Due to this error, the prediction of the wall pressure spectrum is considerably less accurate (see Section 4). However, although it is more accurate, the wall-resolved method is too expensive for use as an everyday design tool. Therefore, an alternative approach based on a semi-analytical model was investigated to predict pressure fluctuations from WMLES data with greater accuracy. Fortunately, the quantities required for this model from the LES are generally fairly well predicted, even near the wall (see Figure 2), which is important because the model is most sensitive to the values near the wall.

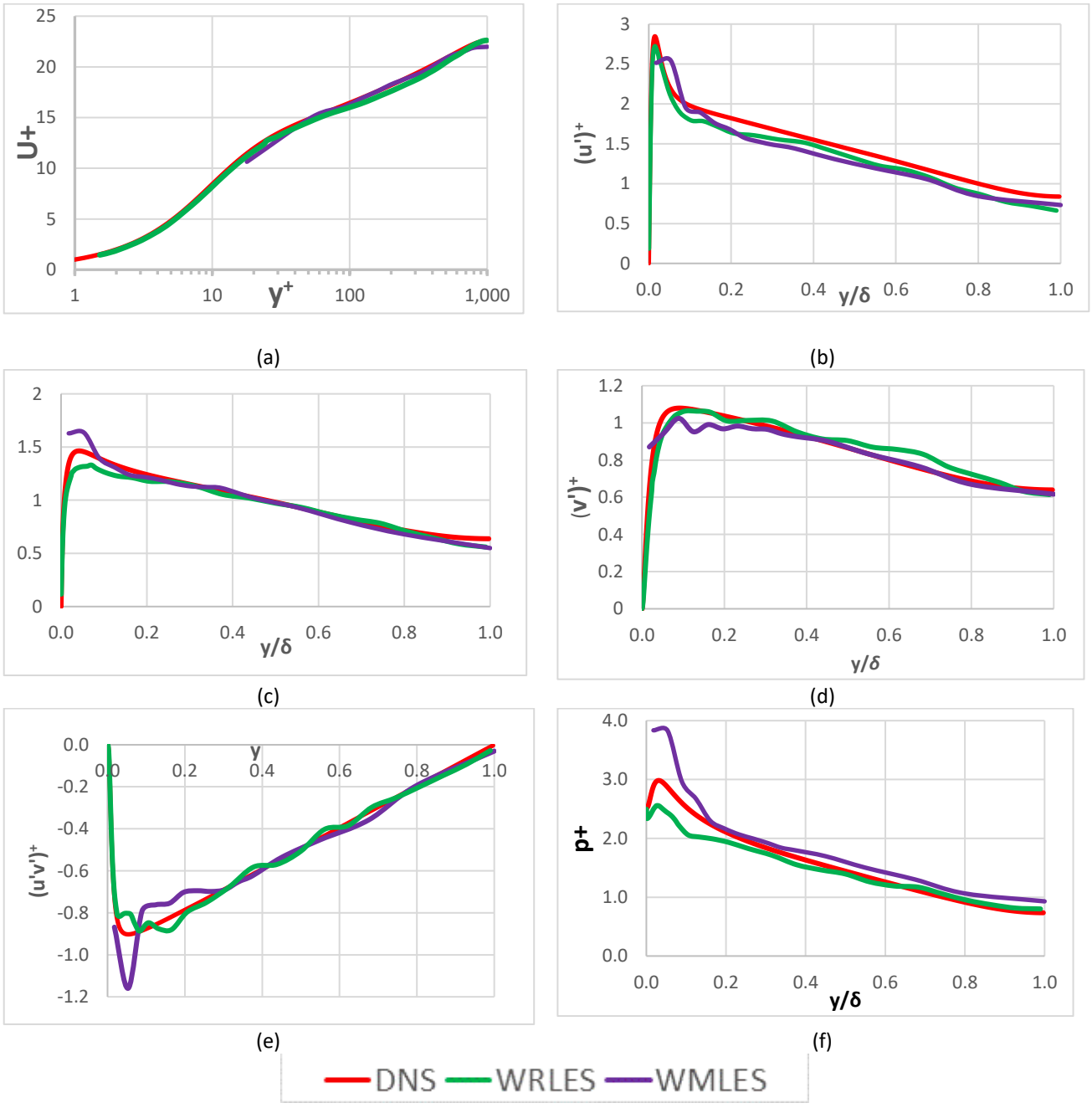

Figure 2 Wall-normal profiles comparing WRLES and WMLES with DNS data for: (a) dimensionless streamwise mean velocity profile; (b) dimensionless r.m.s. streamwise velocity; (c) dimensionless r.m.s. spanwise velocity; (d) dimensionless r.m.s. wall-normal velocity; (e) dimensionless Reynolds shear stress; and (f) dimensionless r.m.s. pressure.

The predictions of fluctuating pressure using WMLES contrast with some other studies using WMLES (as summarised in the Introduction), where good results were obtained near the wall. The explanation must lie in the

differences between the method used here, and the procedures in those studies. One difference is that the wall-adjacent mesh spacing was much finer in some studies, e.g. George and Lele (2016) used a spacing in the wall-normal direction $\Delta y^+ = 7.5$. The use of a finer mesh near surfaces allows for better resolution of the near-wall peak in pressure fluctuations, and allows for extraction of pressure data at a position closer to the wall. Refinement of the mesh near the wall was not used in the current study. However, in some other cases, the wall spacing was more similar to this study, e.g. Park and Moin (2016) used $\Delta y^+ = 20$ (compared to $\Delta y^+ = 18$ in the present study), so mesh spacing may not offer a complete explanation. Another point of difference is that, in all of these other studies, the equation solver treats the fluid as compressible or weakly compressible, whereas the present study assumed incompressible flow. The compressibility assumption substantially changes the way in which the pressure field can be calculated. For incompressible flow, the pressure is obtained by means of a Poisson equation, while compressible solvers do not use this equation. For example, George and Lele (2016) mention that in the Vida code, pressure is obtained using a Helmholtz equation which avoids the numerical stiffness of the Poisson formulation. Thus, compressible fluid solvers may achieve a higher level of accuracy in calculating pressures.

4 APPLICATION OF LES TO ACOUSTICS PREDICTIONS

During each simulation, near-wall pressures were recorded at each time step for each wall, and based on these data the power spectral densities were calculated, following the method of Park and Moin (2016). The resulting spectra are shown in Figure 3(a). The curve for WRLES agrees well with the DNS-based spectrum given by Panton et al. (2017). However, for WMLES, the spectrum is substantially overpredicted, since the pressure fluctuations were overpredicted.

Since the WMLES approach does not seem able to predict near-wall pressure fluctuations accurately, an alternative approach has been investigated as a means to predicting wall pressure fluctuation spectra. A semi-analytical model has been tested (see section 2.3 for description of model). Data for this model were extracted from the simulation results for WRLES and WMLES. The integral length scale was estimated from equations (2) and (4). As shown in Figure 3(b), agreement with DNS data is reasonably good for both WRLES and WMLES. The semi-analytical model is also a more convenient approach to estimate the wall pressure power spectral density compared to the direct approach, since the statistics required for the semi-analytical model will generally converge to steady-state in a shorter simulation compared to the length of simulation required to record pressure data directly and capture a sufficiently wide range of frequencies.

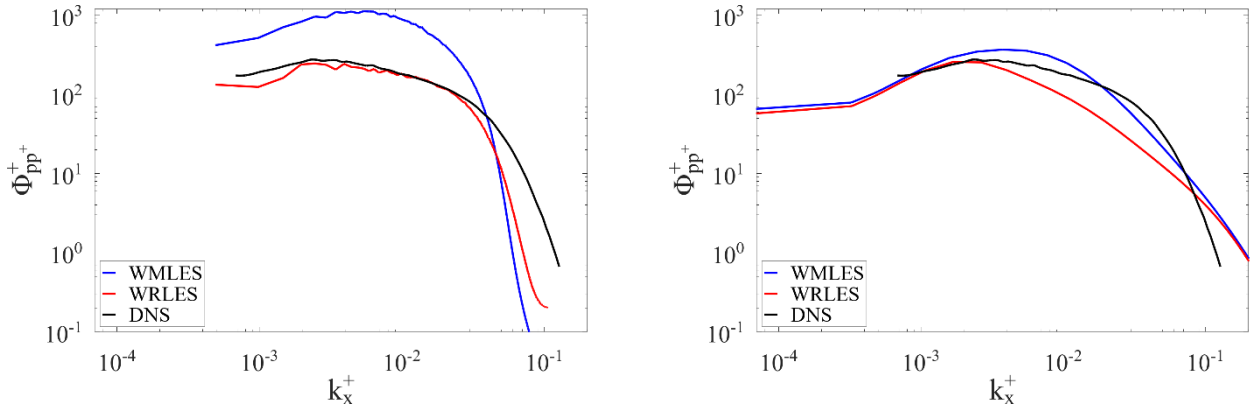

Figure 3 Predictions of dimensionless wall pressure PSD (Φ^+) based on data from WMLES and WRLES and compared with the spectrum obtained directly from DNS (Panton et al., 2017): (a) predictions based on direct use of wall pressure data; (b) predictions based on semi-analytical model.

5 CONCLUSIONS

WRLES and WMLES methods were compared based on turbulent channel flow at a Reynolds number of Re_τ = 1000 using OpenFOAM. It was found that for the mean and r.m.s. velocity statistics, good results could be obtained with a similar level of accuracy with both methods. Using WMLES, however, the computational cost was reduced by more than a factor of 10. Yet, there is a difficulty in applying WMLES results to acoustics predictions, since the near-wall pressure fluctuations showed significant errors. As a consequence, while good results could be obtained using the wall-resolved approach, power spectral density for wall pressure fluctuations was overpredicted with WMLES. An alternative approach to predicting the PSD was tested, based on the semi-analytical

model of Grasso et al. (2019). The inputs to this model consist of other statistics from the LES which are generally better predicted. As a result, good predictions of wall pressure spectra were obtained for both WRLES and WMLES using the semi-analytical model.

ACKNOWLEDGEMENTS
This research was undertaken with the assistance of resources and services from the National Computational Infrastructure (NCI), which is supported by the Australian Government.

REFERENCES

Boukharfane, R., Parsani, M., Bodart, J. (2020). "Characterization of pressure fluctuations within a controlled-diffusion blade boundary layer using the equilibrium wall-modelled LES", *Scientific Reports*, vol. 10:12735.

Carrara, I., 2015, "A-priori Estimation of Turbulent Length Scales for DNS and LES Mesh Guidelines: Application to Backward-facing Step Flow", Thesis, University of Pisa.

Choi, H., Moin, P. (2012). "Grid-point requirements for large eddy simulation: Chapman's estimates revisited", *Phys. Fluids*, vol. 24, 011702.

George, K.J., Lele, S.K. (2016). "Large-eddy simulation of airfoil self-noise at high Reynolds number", *AIAA Paper* 2016-2919, 22nd AIAA/CEAS Aeroacoustics Conference, Lyon, France.

Grasso, G., Jaiswal, P., Wu, H., Moreau., S., Roger, M. (2019). "Analytical models of the wall-pressure spectrum under a turbulent boundary layer with adverse pressure gradient", *J Fluid Mech*, vol. 877, pp. 1007–1062.

Kamruzzaman, M., Lutz, T., Würz, W., Krämer, E. (2011). "On the length scales of turbulence for aeroacoustic applications". *Proc. 17th AIAA/CEAS Aeroacoustic Conference*.

Komen, E.M.J., Camilo, L.H., Shams, A., Geurts, B.J., Koren, B. (2017). "A quantification method for numerical dissipation in quasi-DNS and under-resolved DNS, and effects of numerical dissipation in quasi-DNS and under-resolved DNS of turbulent channel flows", *J. Comput. Physics*, vol.345, pp. 565–595.

Larsson, J., Kawai, S., Bodart, J., Bermejo-Moreno, I., (2016). "Large eddy simulation with modelled wall-stress: recent progress and future directions", *Mech. Eng. Rev.*, *Bulletin of the JSME*, vol. 3(1).

Lee M., Moser R.D. (2015). "Direct numerical simulation of turbulent channel flow up to Re_tau = 5200", *J. Fluid Mech*., vol. 774, pp. 395–415.

Mehrabadi, M., Bodony D.J., 2019, "Wall-Modeled Large-Eddy Simulation and Direct Numerical Simulation of Broadband Trailing Edge Noise from a NACA0012 Airfoil", *25th AIAA/CEAS Aeroacoustics Conference*, 20-23 May 2019, Delft, The Netherlands.

Michel, R., Quemard, C., Durant, R. (1968). "Hypotheses on the mixing length and application to the calculation of turbulent boundary layers". In: *Proc. Computation Turb. Boundary Layers,* vol. 1 pp. 195 – 207 (Kline, S.J. et al., eds.).

Mukha, T., Rezaeiravesh, S , Liefvendahl, M. (2019). "A library for wall-modelled large-eddy simulation based on OpenFOAM technology", *Comput. Phys. Commun.*, vol. 239, pp. 209–224.

Nicoud F., Ducros, F., (1999). "Subgrid-scale stress modelling based on the square of the velocity gradient tensor". *Flow Turbul. Combust*., vol. 62(3), pp.183–200.

Panton, R. L., Linebarger, J. H. (1974). "Wall pressure spectra calculations for equilibrium boundary layers", *J. Fluid Mech*., vol. 65 (02), pp. 261–287.

Panton, R.L., Lee, M., Moser, R.D. (2017). "Correlation of pressure fluctuations in turbulent wall layers", *Physical Review Fluids*, **2**, 094604.

Park, G.I., Moin, P. (2016). "Space-time characteristics of wall-pressure and wall shear-stress fluctuations in wall-modeled large eddy simulation", *Phys. Rev. Fluids*, vol. 1, 024404.

Pérez Arroyo, C., Leonard, T., Sanjosé, M., Moreau, S., Duchaine, F. (2019). "Large Eddy Simulation of a scale-model turbofan for fan noise source diagnostic", *J. Sound Vibration*, vol. 445, pp. 64–76.

Pope, S.B. (2000). *Turbulent flows*, Cambridge Universiy Press.

Rezaeiravesh, S., Mukha, T., Liefvendahl, M. (2019). "Systematic study of accuracy of wall-modeled large eddy simulation using uncertainty quantification techniques", *Comput. Fluids*, vol. 185, pp. 34–58.

Spalding, DB. 1961. 'A Single Formula for the Law of the Wall'. *Transactions of the ASME Journal of Applied. Mechanics*, vol. 28, p. 455.

Wilcox, D.C. (1993). *Turbulence Modeling for CFD*, DCW Industries, Inc., California, USA.

Winkler, J., Wu, H., Moreau, S., Carolus, T., Sandberg, R.D. (2020). "Trailing-edge broadband noise prediction of an airfoil with boundary-layer tripping", *J. Sound Vibration*, vol. 482, 115450.

Wolf, W.R., Lele, S.K. (2012). "Trailing-Edge Noise Predictions Using Compressible Large-Eddy Simulation and Acoustic Analogy", *AIAA J.*, vol. 50(11).